

Supporting Information

**Silicon/graphite composite anode with constrained swelling and stable solid
electrolyte interphase enabled by spent graphite**

Qi Xu,^a Qianwen Wang,^a Dequan Chen,^a Yanjun Zhong,^a Zhenguo Wu,^{*a} Yang

Song,^a Gongke Wang,^b Yuxia Liu,^c Benhe Zhong^a and Xiaodong Guo^a

^a*School of Chemical Engineering, Sichuan University, Chengdu 610065, P. R. China*

^b*School of Materials Science and Engineering, Henan Normal University, XinXiang
453007, P. R. China*

^c*School of Chemistry and Chemical Engineering, Qufu Normal University, Qufu
273165, P. R. China.*

**Corresponding author:*

E-mail address: zhenguowu@scu.edu.cn

Table S1 Crystal plane spacings of (002) peaks in AG and SG.

| Samples | $2\theta_{(002)}$ ($^{\circ}$) | $d_{(002)}$ (nm) |
|---------|----------------------------------|------------------|
| AG | 26.288 | 0.3387 |
| SG | 26.235 | 0.3394 |

Table S2 Surface element distributions of AG and SG.

| Samples | C (%) | O (%) | Li (%) | F (%) | P (%) |
|---------|-------|-------|--------|-------|-------|
| AG | 98.05 | 1.95 | / | / | / |
| SG | 94.72 | 3.33 | 1.49 | 0.33 | 0.14 |

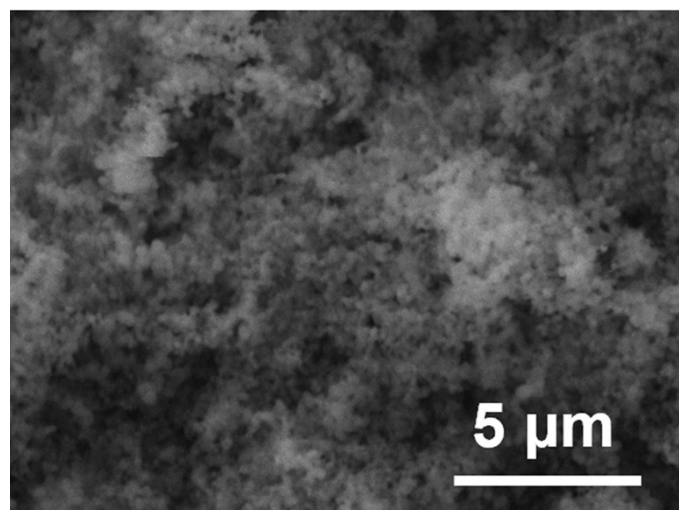


Fig. S1 SEM image of Si nanoparticles.

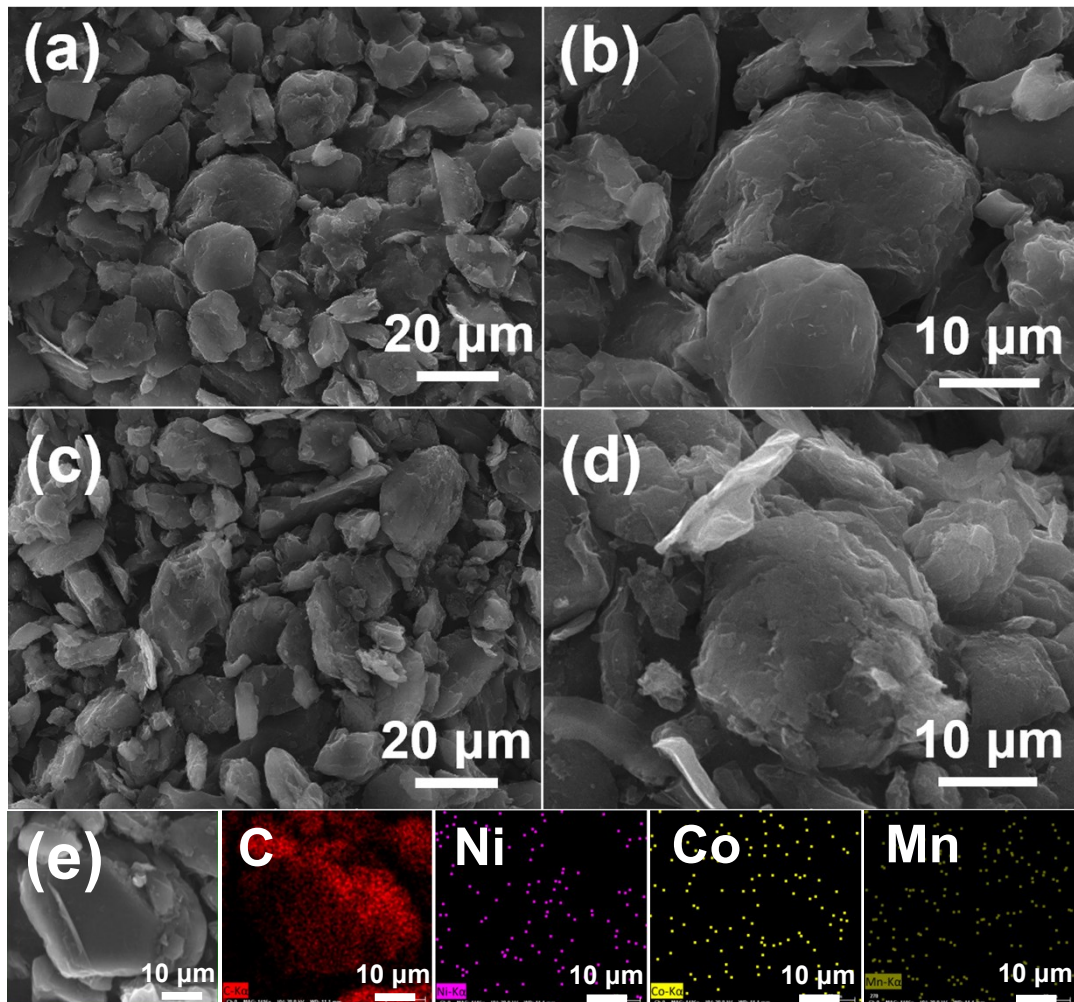


Fig. S2 SEM images of (a-b) AG and (c-d) SG, (e) corresponding EDS mapping images of SG.

Table S3 ICP-OES results of SG.

| Elements | Li | Ni | Co | Mn | Al | Cu | Fe |
|---------------|--------|--------|-------|--------|--------|--------|--------|
| Content (ppm) | 266.29 | 215.05 | 75.33 | 365.88 | 137.20 | 139.21 | 120.79 |

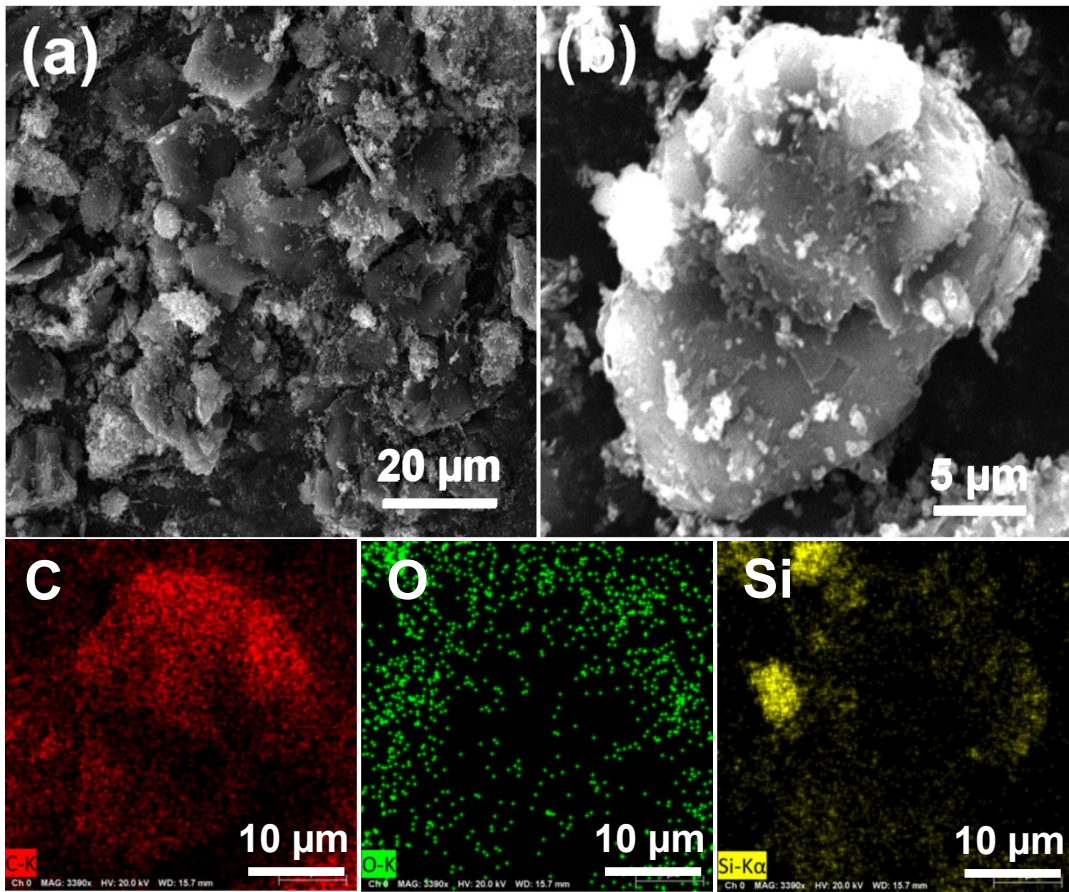


Fig. S3 (a) SEM image and (b) corresponding EDS mapping images of Si/AG composite.

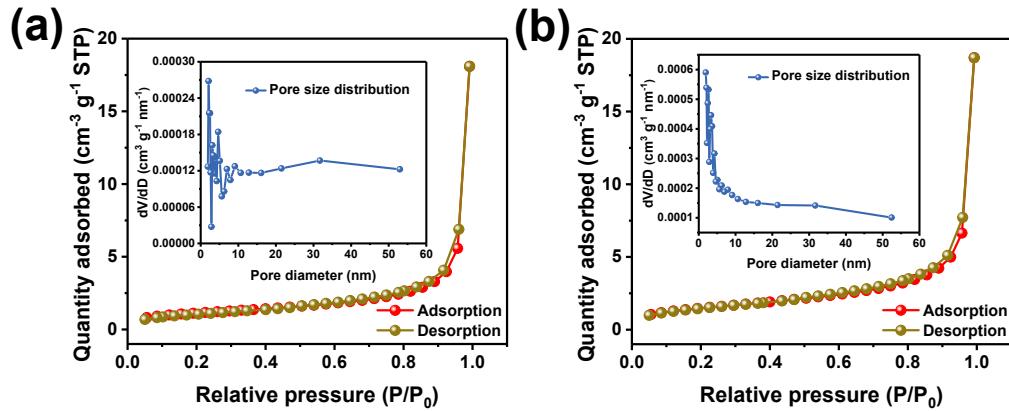


Fig. S4 Nitrogen adsorption-desorption isotherms and corresponding pore size distributions of (a) Si/AG and (b) Si/SG composites.

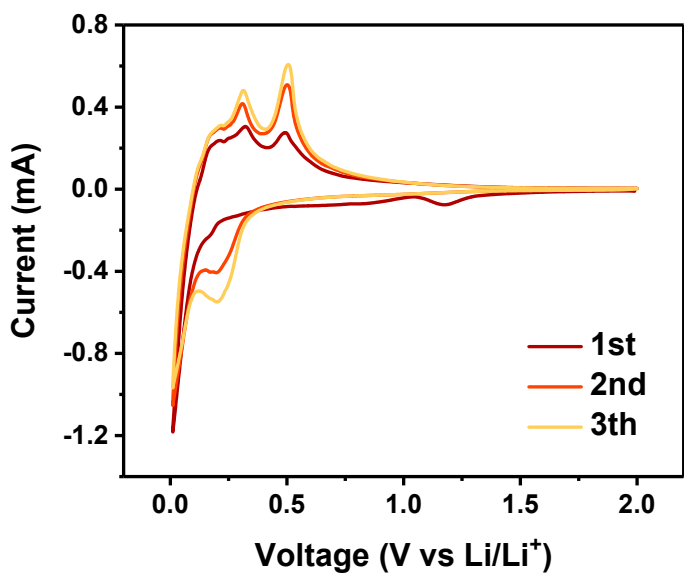


Fig. S5 CV curves of Si/AG composite at a scan rate of 0.1 mV s^{-1} for the first three cycles.

Table S4 Comparison of electrochemical performance with the other Si/graphite anodes in recent reported literatures.

| Anodes | Synthesis strategy | Si content (wt%) | Mass loading (g cm^{-2}) | ICE (%) | Cycling stability (mAh g^{-1}) | Rate capacity (mAh g^{-1}) |
|---|-----------------------------|------------------|-------------------------------------|---------|---|---------------------------------------|
| $\text{Si}_{\text{FS}}/\text{G}@\text{C}_1$ | Ball milling | 25 | / | 76.3 | 730 after 100 cycles at 0.1 A g^{-1} | $\sim 680, 1 \text{ A g}^{-1}$ |
| SiGC^2 | Ball milling + spray drying | 12.8 | 1.1 | 80.5 | 610 after 300 cycles at 0.5 A g^{-1} | $458, 2 \text{ A g}^{-1}$ |
| CSG^3 | CVD | 16.8 | 1.0-1.05 | 80.5 | 530 after 100 cycles at 0.074 A g^{-1} | $260, 1.86 \text{ A g}^{-1}$ |
| Si/C-AG^4 | Ball milling | 21.5 | 1 | 64 | 334 after 500 cycles at 1 A g^{-1} | $350, 2 \text{ A g}^{-1}$ |
| c-Gr + 15% Si ⁵ | Calcination + etching | 15.4 | 0.9-1.1 | 74.2 | 485 after 400 cycles at 1 A g^{-1} | $770, 2 \text{ A g}^{-1}$ |
| Nano-Si/G/C-2 ⁶ | Ball milling | 15.4 | 0.968 | 83 | 368 after 500 cycles at 1 A g^{-1} | $200, 4 \text{ A g}^{-1}$ |
| GSiWh^7 | Ball milling | 33.3 | 1.4 | 74 | 595 after 200 cycles at 2 A g^{-1} | $500, 0.5 \text{ A g}^{-1}$ |
| $\text{Si/G}@\text{C}^8$ | Ball milling | 24.5 | 0.95 | 83.7 | ~ 630 after 180 cycles at 0.2 A g^{-1} | $697, 1 \text{ A g}^{-1}$ |
| MSC-2 ⁹ | Magnesiothermic reduction | 21 | 2 | 81.3 | 648 after 105 cycles at 0.1 A g^{-1} | $218, 1.5 \text{ A g}^{-1}$ |
| Si/G/C^{10} | Electrospray + ball milling | 21.8 | / | 56.3 | 400 after 200 cycles at 0.5 A g^{-1} | $538, 2 \text{ A g}^{-1}$ |
| This work | Ball milling | 32.6 | 1.0-1.3 | 76.4 | 562 after 400 cycles at 1 A g^{-1} | $646, 3 \text{ A g}^{-1}$ |

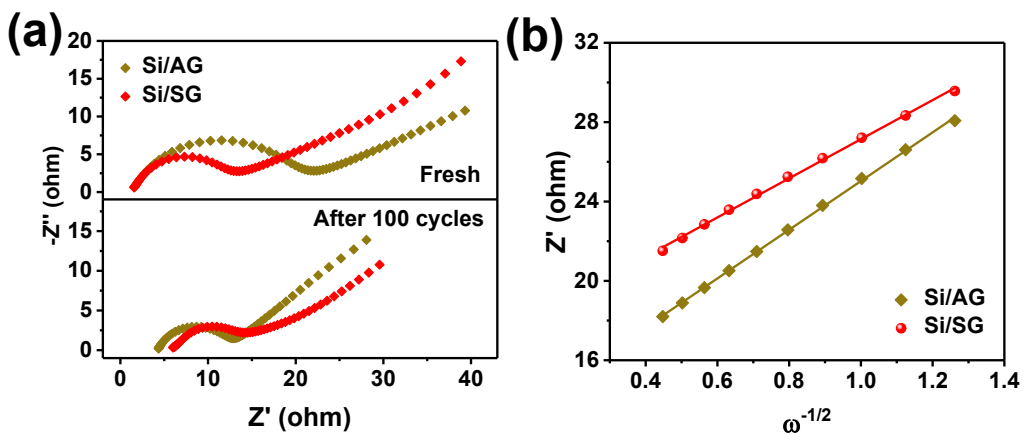


Fig. S6 (a) Nyquist plots of Si/AG and Si/SG composite electrodes before and after 100 cycles and (b) corresponding linear fits (relationship between Z' and $\omega^{-1/2}$) in the low-

frequency region after 100 cycles.

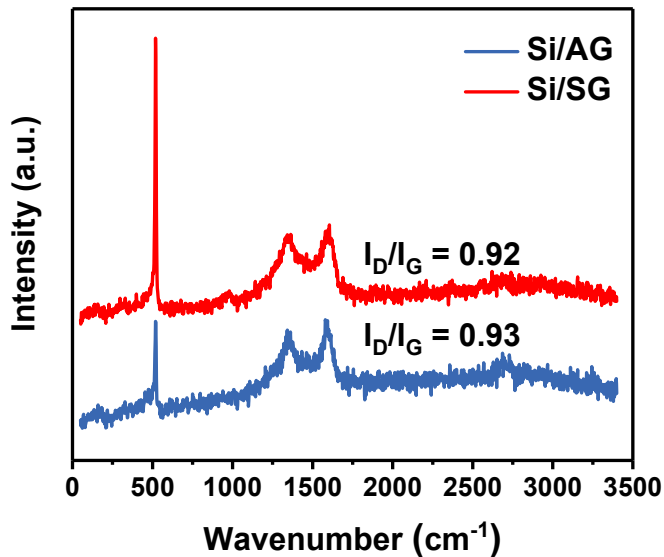


Fig. S7 Raman spectra of cycled Si/AG and Si/SG composite electrodes.

Table S5 Surface element distributions of Si/AG and Si/SG electrodes after 3 cycles.

| Samples | C (%) | O (%) | Li (%) | F (%) | Si (%) |
|---------|-------|-------|--------|-------|--------|
| Si/AG | 47.53 | 29.61 | 19.1 | 2.85 | 0.89 |
| Si/SG | 49.14 | 30.12 | 17.87 | 2.04 | 0.83 |

References

- 1 L. Geng, D. Yang, S. Gao, Z. Zhang, F. Sun, Y. Pan, S. Li, X. Li, P.-F. Cao and H. Yang, *Adv. Mater. Interfaces*, 2020, **7**, 1901726.
- 2 D. Sui, Y. Xie, W. Zhao, H. Zhang, Y. Zhou, X. Qin, Y. Ma, Y. Yang and Y. Chen, *J. Power Sources*, 2018, **384**, 328-333.
- 3 B. Liu, P. Huang, Q. Zhang, Q. Huang and Z. Xie, *J Mater Sci*, 2020, **55**, 12165-12176.
- 4 W. Yang, H. Ying, S. Zhang, R. Guo, J. Wang and W.-Q. Han, *Electrochim. Acta*, 2020, **337**, 135687.
- 5 M. Chen, W. Cao, L. Wang, X. Ma and K. Han, *ACS Appl. Energy Mater.*, 2021, **4**,

- 775-783.
- 6 A. Sun, H. Zhong, X. Zhou, J. Tang, M. Jia, F. Cheng, Q. Wang and J. Yang, *Appl. Surf. Sci.*, 2019, **470**, 454-461.
 - 7 M. H. Parekh, V. P. Parikh, P. J. Kim, S. Misra, Z. Qi, H. Wang and V. G. Pol, *Carbon*, 2019, **148**, 36-43.
 - 8 T. Mu, Z. Zhang, Q. Li, S. Lou, P. Zuo, C. Du and G. Yin, *J. Colloid Interface Sci.*, 2019, **555**, 783-790.
 - 9 P. Fan, T. Mu, S. Lou, X. Cheng, Y. Gao, C. Du, P. Zuo, Y. Ma and G. Yin, *Electrochim. Acta*, 2019, **306**, 590-598.
 - 10 W. Liu, Y. Zhong, S. Yang, S. Zhang, X. Yu, H. Wang, Q. Li, J. Li, X. Cai and Y. Fang, *Sustain. Energy Fuels*, 2018, **2**, 679-687.